

# Effect of Tertiary and Secondary Phosphines on Low-Temperature Formation of Quantum Dots\*\*

Kui Yu,\* Xiangyang Liu, Qun Zeng, Donald M. Leek, Jianying Ouyang, Kenneth Matthew Whitmore, John A. Ripmeester, Ye Tao, and Mingli Yang\*

The cost, reaction temperature, particle yield, and synthetic reproducibility of colloidal semiconductor quantum dots (QDs) are the enduring issues for these materials to reach their full potential.<sup>[1–9]</sup> Herein, using the reaction of cadmium oleate ( $\text{Cd}(\text{OA})_2$  or  $\text{Cd}(\text{OOC}\text{C}_{17}\text{H}_{33})_2$ ) and tri-*n*-octylphosphine selenide (SeTOP or  $\text{Se}=\text{P}(\text{C}_8\text{H}_{17})_3$ ) to produce CdSe nanocrystals (NCs) as a model system, we demonstrated that together with high Cd-to-Se and Se-to-TOP feed molar ratios, the use of a small amount of a secondary phosphine, commercial diphenylphosphine (DPP or  $\text{PPh}_2\text{H}$ ), offers a practical means to overcome these challenges: particle yield and synthetic reproducibility were greatly enhanced at lower reaction temperatures. For the reaction of  $\text{Cd}(\text{OA})_2 + \text{SeTOP} + \text{DPP}$ , in situ  $^{31}\text{P}$  NMR and density functional theory (DFT) calculations suggested that it is SeDPP rather than SeTOP that reacts with  $\text{Cd}(\text{OA})_2$  at low temperature, leading to the formation of the CdSe NCs. The facile coordination of TOP instead of DPP to  $\text{Cd}(\text{OA})_2$  conveys the subtle chemistry of the tertiary and secondary phosphines affecting the formation of the NCs: the equilibrium of  $\text{SeTOP} + \text{DPP} \rightleftharpoons \text{TOP} + \text{SeDPP}$  is weighted toward SeTOP, but high Cd-to-Se and Se-to-TOP feed molar ratios drive the equilibrium toward SeDPP. The reactivity of SeDPP is much higher than that of SeTOP. We postulate herein a probable chemical mechanism for the reaction of  $\text{Cd}(\text{OA})_2 + \text{SeDPP}$ : the release of acid  $\text{C}_{17}\text{H}_{33}\text{COOH}$  from  $(\text{OA})_2\text{Cd}(\text{Se}=\text{PPh}_2\text{H})_2$  followed by the release of  $\text{PPh}_2\text{H}$  from  $(\text{OA})\text{Cd}(\text{Se}=\text{PPh}_2)(\text{Se}=\text{PPh}_2\text{H})$  by way of cleavage of the  $\text{Se}=\text{P}$  bond of the  $\text{Se}=\text{PPh}_2\text{H}$  arm. With a small amount of secondary phosphines and with high

Cd-to-Se and Se-to-TOP feed molar ratios, the enduring issues for the synthesis of colloidal semiconductor QDs can be overcome.

Colloidal semiconductor QDs have been the focus of much research, from basic science to applied technologies.<sup>[1,2]</sup> Many methods have been developed to improve the control of NC size, size distribution, and shape,<sup>[3–18]</sup> with a few also addressing particle yield and synthetic reproducibility.<sup>[6–9]</sup> Motivated by a need for a higher degree of synthetic control, more rational design and lower cost for NCs of high quality,<sup>[2]</sup> some efforts were made to understand the formation mechanism of monomers (such as from the reaction of  $\text{Cd}(\text{OA})_2 + \text{SeTOP}$ ).<sup>[10]</sup>

There has only been limited improvement of the wet-chemical synthesis of colloidal NCs for the past decade despite the great flexibility of the reactions involved.<sup>[3–18]</sup> For example, the definitive precursors in the synthesis of II–VI NCs have now been determined, mainly, to be metal alkylcarboxylates, such as cadmium oleate ( $\text{Cd}(\text{OA})_2$ ), and trialkylphosphine chalcogenides, such as SeTOP. To promote the particle yield of PbSe NCs, Bawendi and co-workers pioneered the use of a secondary phosphine, commercial diphenylphosphine (DPP), as an additive in 2006.<sup>[6]</sup> In that case,  $\text{Pb}(\text{OA})_2$ , SeTOP, and DPP were mixed in 1-octadecene (ODE), with low Pb-to-Se feed molar ratios, such as 1:5 and 1M SeTOP made from elemental Se or commercial TOP with a feed molar ratio of 1:2.2.<sup>[6]</sup> Two reaction paths for the formation of PbSe monomers were proposed: one was the reaction of  $\text{Pb}(\text{OA})_2$  and SeTOP and the other was the reaction of metallic  $\text{Pb}^0$  (from the reduction of  $\text{Pb}(\text{OA})_2$  by DPP) and  $\text{Se}^0$  (released from SeTOP).

Krauss and co-workers articulated a completely different role for DPP in 2010.<sup>[8]</sup> They claimed that the formation of  $\text{Pb}^0$  was unlikely at low reaction temperatures and  $\text{Pb}^0$  had little reactivity towards SeTOP. Instead, they proposed the formation of SeDPP by way of Se exchange from SeTOP to DPP. They stated that SeTOP was inert toward metal carboxylates and was only a soluble Se source. Without the addition of DPP, they designated that dioctylphosphine selenide (SeDOP) represented the very reactive species responsible for the formation of PbSe NCs at low temperature.

DOP, another secondary phosphine, was acknowledged as one important impurity in commercial 90 % TOP and possibly in 97 % TOP.<sup>[7,8,12,13,14b,17]</sup> The amount of DOP in commercial TOP may vary from batch to batch; such batch-to-batch variation was correlated to the problems of low particle yield and low synthetic reproducibility. At the beginning of 2012,<sup>[17]</sup> Wang and Buhro reported that the formation of CdSe QDs, instead of nanorods, was favored by the addition of DOP to

[\*] Dr. K. Yu, Dr. X. Liu, D. M. Leek, Dr. J. Ouyang, K. M. Whitmore, Dr. J. A. Ripmeester, Dr. Y. Tao  
National Research Council of Canada  
Ottawa, ON, K1A 0R6 (Canada)  
E-mail: kui.yu@nrc-cnrc.gc.ca

Q. Zeng, Prof. M. Yang  
Institute of Atomic and Molecular Physics and State Key Laboratory of Biotherapy  
Sichuan University, Chengdu 610065 (P. R. China)  
E-mail: myang@scu.edu.cn

[\*\*] We thank Dr. Hong Cao for some of the in situ absorption measurements presented, Kenneth Chan for the MALDI measurement, Dr. Dennis Whitfield and Dr. Keith Ingold for useful discussions, Donald Van Loon and Vivier Lefebvre for financial support, and the Defence Research and Development Canada Centre for Security Science Chemical, Biological, Radiological/Nuclear, and Explosives Research and Technology Initiative (CRTI 09-0511RD “Next-generation stand-off radiation detection using nanosensors”) for financial support.

Supporting information for this article is available on the WWW under <http://dx.doi.org/10.1002/ange.201300568>.

the reaction of cadmium alkylphosphonates and SeTOP, where DOP was synthesized in situ and is not commercially available. The presence of DOP was believed to promote the reactivity between the Cd and Se precursors appreciably.<sup>[17]</sup>

A similar strategy was used with commercial DPP<sup>[6]</sup> to synthesize various NCs, such as PbSe,<sup>[7–9,12]</sup> CdSe,<sup>[8,11]</sup> ZnSe,<sup>[13]</sup> PbSeS,<sup>[14]</sup> ZnSeS,<sup>[15]</sup> and CuInS<sub>2</sub>.<sup>[16]</sup> Improvements in the yield of small PbSe QDs (with a band-gap of 1239 nm) have been made with the use of DPP and a high feed molar ratio of 4Pb(OA)<sub>2</sub>:1SeTOP;<sup>[9]</sup> with the use of DPP but a lower feed molar ratio (1Pb(OA)<sub>2</sub>:5SeTOP), the yield of PbSe QDs (with a band-gap of 1716 nm) was only approximately 16%.<sup>[6]</sup> The combination of DPP and high Pb-to-Se feed molar ratios was the key to high reaction yields, particularly for small QDs.<sup>[9]</sup> SeTOP has been used as the phosphine chalcogenide precursor in standard QD syntheses, and the chemistry of the tertiary and secondary phosphines is still remains inconclusive. The lack of a rational synthetic mechanism, including mechanisms for Se=P bond cleavage of SeTOP and SeDPP leading to the formation of monomers, has delayed the advance of design and synthesis of colloidal QDs.<sup>[8,18]</sup> Herein, we have studied the effect of the tertiary and secondary phosphines on low-temperature nucleation/growth with enhanced particle yield and synthetic reproducibility. With insight into the phosphine chemistry, we provide a conceptual method for the rational design of low-temperature, low-cost production of high-quality colloidal NCs, with high reproducibility and yield.

Equation (1) illustrates our model reaction system of Cd(OA)<sub>2</sub> and SeTOP in ODE at low temperature with the addition of DPP.

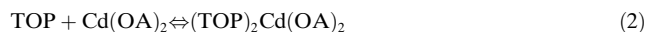


The presence of DOP in commercial 90% and 97% TOP is shown in Figure S1A (see Supporting Information). Note that DOP was not detected in 97% TOP in a previous study.<sup>[17]</sup> Thus, the amount of DOP in commercial TOP changes from batch to batch. The difference between the DOP amounts of 90% and 97% TOP should be larger than the variation between two batches of either 90% or 97% TOP. Thus, we used 90% and 97% TOP to verify the ability of DPP to promote synthetic reproducibility.

Figure S1B shows the temporal evolution of the absorption of growing CdSe NCs in ODE from five pairs of ten batches with and without DPP; SeTOP was made from commercial 90% and 97% TOP. Without DPP, SeTOP made from 90% TOP is more reactive than that made from 97% TOP. With DPP, the formation of the CdSe NCs was much favored at lower reaction temperatures along with giving a higher yield and reproducibility; high Se-to-TOP feed molar ratios to limit the presence of TOP were also preferred. For the batches with the 4Cd:1Se:2.2TOP feed molar ratios, the size of the particles formed was insensitive to the amounts of DPP used (Figure S1C). Figure S1D shows a slower rate of nucleation in the presence of a large amount of TOP.

With high Cd-to-Se and Se-to-TOP feed molar ratios, the addition of commercial DPP can be used for efficient NC synthesis at low cost, high yield, and good reproducibility at

low reaction temperatures.<sup>[9,12,13]</sup> Note that high-quality colloidal NCs were produced at low reaction temperatures when there was high reactivity of the precursors.<sup>[9,13,14b,15]</sup> Such a requirement on high Cd-to-Se and Se-to-TOP feed molar ratios could be attributed to the coordination of TOP instead of DPP toward Cd(OA)<sub>2</sub> (shown in Equation (2)) and the equilibrium shown in Equation (3).



The coordination of Se=P(C<sub>6</sub>H<sub>17</sub>)<sub>3</sub> and Se=PPh<sub>2</sub>H to M(OA)<sub>2</sub> (M = Cd or Pb) was suggested,<sup>[6,8,10]</sup> but no one has addressed the coordination of TOP to Cd(OA)<sub>2</sub>. Such coordination is critical to drive the equilibrium of Equation (3) to the right: with high Cd-to-Se and Se-to-TOP feed molar ratios, Cd(OA)<sub>2</sub> can consume free TOP (Equation (2)) from the SeTOP solution, together with what is produced from Equation (3) after the Se exchange from TOP to DPP. Figure 1 shows the coordination of TOP and/or DPP towards Cd(OA)<sub>2</sub>. TOP exhibited much higher coordination capability than DPP. Figure 1A and Figure S2A illustrate our DFT calculations on the coordination of Cd(OAc)<sub>2</sub> with tertiary and secondary phosphines of trimethylphosphine (TMP) and DPP, respectively. This calculation suggests a similar interaction pattern, namely the P atom in the phosphines attacking directly the Cd in Cd(OAc)<sub>2</sub>. See Table S2A for calculations of the relative energy ( $\Delta E$ ) and Gibbs free energy ( $\Delta G$ ) for the Cd(OAc)<sub>2</sub> coordination with PPh<sub>2</sub>H, (CH<sub>3</sub>)<sub>2</sub>PH, or (CH<sub>3</sub>)<sub>3</sub>P. Note that these reactions are barrier-free but have  $\Delta G$  values of 25.04 kJ mol<sup>−1</sup>, 9.87 kJ mol<sup>−1</sup>, and −1.45 kJ mol<sup>−1</sup> for PPh<sub>2</sub>H, (CH<sub>3</sub>)<sub>2</sub>PH, and (CH<sub>3</sub>)<sub>3</sub>P, respectively. Accordingly, the Cd(OA)<sub>2</sub> coordination with the tertiary phosphine TOP should proceed more easily than with the secondary phosphine PPh<sub>2</sub>H. This result is noteworthy and was supported by our in situ <sup>31</sup>P NMR spectroscopy experiments.

Figure 1B shows in situ <sup>31</sup>P NMR spectra from five mixtures and 90% TOP at different temperatures. The mixtures were 1Cd(OA)<sub>2</sub>:6TOP, 1Cd(OA)<sub>2</sub>:3TOP, 2Cd(OA)<sub>2</sub>:1TOP, 2Cd(OA)<sub>2</sub>:1TOP:1DPP, and 1Cd(OA)<sub>2</sub>:1DPP. For the first four mixtures, the P resonance of TOP (−32 ppm) disappeared upon mixing at room temperature (25 °C), and a relatively low-field signal was detected, the chemical shift of which was affected by the amount of TOP used. For example, one P resonance at −25 ppm was detected for the mixture 1Cd(OA)<sub>2</sub>:6TOP, at −19 ppm with 1Cd(OA)<sub>2</sub>:3TOP, and at −9 ppm with 2Cd(OA)<sub>2</sub>:1TOP. The more TOP that was present, the larger the high-field signal was (closer to the P resonance (−32 ppm) of free TOP). Probably, the single P resonance signal detected at 25 °C (1:6) and at 80 °C (1:6) represents an averaged chemical shift of both free TOP (−32 ppm) and coordinated TOP (−10 ppm).<sup>[19]</sup>

Accordingly, when the four mixtures were cooled to −55 °C (Figure 1B, bottom left), there were two P signals detected at approximately −10 ppm and −33 ppm. The chemical shift of TOP at −55 °C was −33 ppm. For example, when the 1Cd(OA)<sub>2</sub>:3TOP mixture was cooled to −55 °C

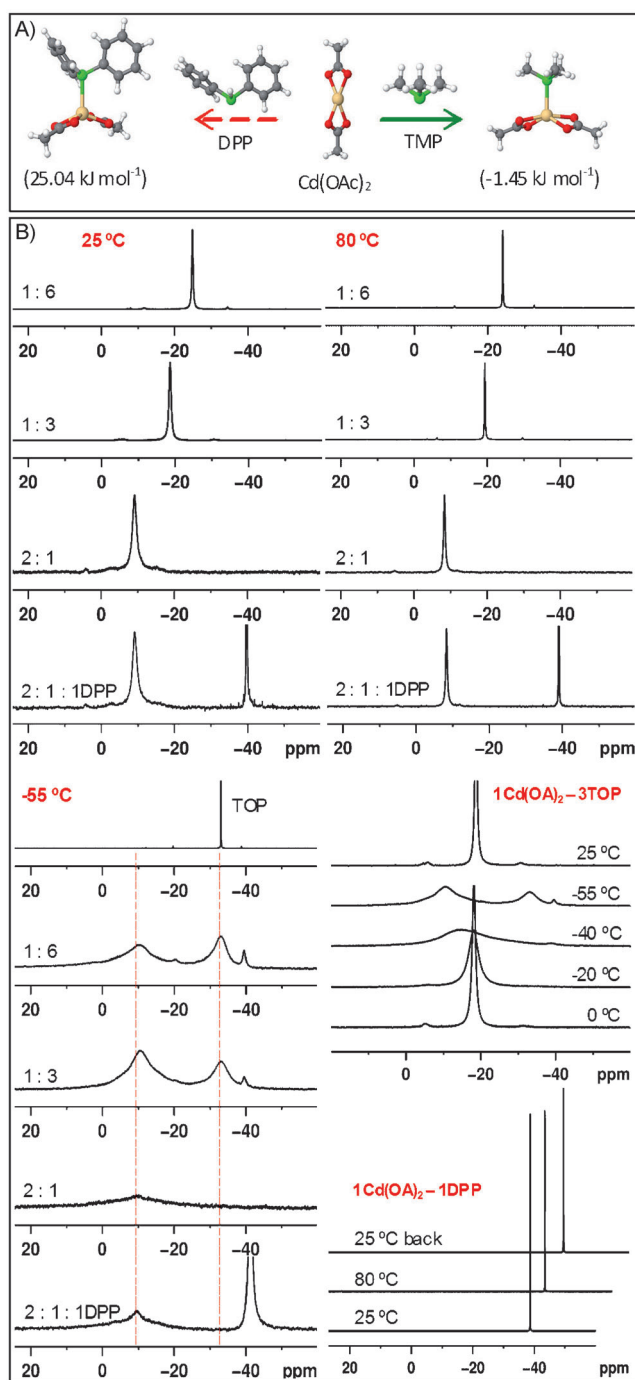


**Figure 1.** A) DFT calculations of the coordination between  $\text{Cd}(\text{OAc})_2$  and TOP or DPP (Cd yellow; P green; C gray; H white; O red). The calculated changes in Gibbs free energy are shown in parentheses. B) In situ  $^{31}\text{P}$  NMR spectra of the coordination from five mixtures of  $\text{Cd}(\text{OAc})_2$  (X) and TOP (Y) and/or DPP (Z) with the different feed molar ratios (in the form X:Y:Z) and at the temperatures indicated. Also, the  $^{31}\text{P}$  NMR spectra of TOP at  $-55^\circ\text{C}$  is shown.

(Figure 1B, middle right), the signal broadened from  $0^\circ\text{C}$  to  $-40^\circ\text{C}$ ; two signals emerged at  $-55^\circ\text{C}$ . When the temperature was re-elevated to  $25^\circ\text{C}$ , a single resonance was recovered at the same chemical shift as from before cooling. Subsequently, an equilibrium between TOP and a  $\text{Cd-P}(\text{C}_8\text{H}_{17})_3$  complex, seems to exist even at low temperature

( $-40^\circ\text{C}$  and above). The formation of such a  $\text{Cd-P}(\text{C}_8\text{H}_{17})_3$  complex should be facile. The in situ  $^{31}\text{P}$  NMR study shows a classical chemical exchange for the coordination of TOP to  $\text{Cd}(\text{OAc})_2$ :<sup>[19]</sup> the spectra become sensitive to the exchange when the exchange rate becomes similar to the frequency difference between the signals, and the exchange slows down at low temperature. Figure S2B shows MALDI mass spectra of a mixture of  $1\text{Cd}(\text{OAc})_2:3\text{TOP}$ , suggesting that this complex is of the form of  $\text{Cd}(\text{OAc})_2(\text{TOP})_2$ .

Little coordination was revealed from the mixture of  $1\text{Cd}(\text{OAc})_2:1\text{DPP}$  at  $25^\circ\text{C}$ , when heated to  $80^\circ\text{C}$  and then cooled to  $25^\circ\text{C}$  (Figure 1B, bottom right). Only the P resonance of free DPP ( $-40 \text{ ppm}$ ) was detected from various mixtures of  $\text{Cd}(\text{OAc})_2$  and DPP. Even after three hours at  $140^\circ\text{C}$ , our  $1\text{Cd}(\text{OAc})_2:1.3\text{DPP}$  mixture did not exhibit any  $\text{Cd}^0$  precipitation, and little change of DPP was detected (Figure S2C).

TOP is a better donor ligand than DPP for the coordination toward  $\text{Cd}(\text{OAc})_2$ . The P atom of  $\text{P}(\text{C}_8\text{H}_{17})_3$  has larger condensed nucleophilic softness than that of  $\text{PPh}_2\text{H}$ . See Table S2B for the calculation of the softness, a DFT descriptor used to assess atomic reactivity.<sup>[20,21]</sup> The P atom of TMP has greater condensed softness than that of DPP; thus, TMP is more nucleophilic than DPP.

For Equation (3), DFT and in situ  $^{31}\text{P}$  NMR studies are shown in Figure S3A. With a calculated equilibrium constant of  $6.76 \times 10^{-4}$  and activation energy of  $119.22 \text{ kJ mol}^{-1}$ , the equilibrium was weighted toward SeTOP. Calculations of  $\Delta E$  and  $\Delta G$  (Table S3) confirm the probable exchange of Se between TMP and DPP or between TMP and DMP. The  $\text{TMPSe} + \text{DPP}$  or  $\text{TMPSe} + \text{DMP}$  reactants have a lower  $\Delta G$  ( $27.32 \text{ kJ mol}^{-1}$  or  $14.81 \text{ kJ mol}^{-1}$ ) than the  $\text{TMP} + \text{SeDPP}$  or  $\text{TMP} + \text{SeDMP}$  products, respectively.  $\text{Se=PPh}_2\text{H}$  at approximately  $7.2 \text{ ppm}$  was not detected in  $4\text{DPP}:1\text{Se}:2.2\text{TOP}$  but was detected in  $4\text{DPP}:1.2\text{Se}:1\text{TOP}$  (Figure S3A). This SeTOP made from  $1.2\text{Se}:1\text{TOP}$  was filtered before use and is called pure SeTOP. Free TOP was found in  $1\text{M}$  SeTOP but not in pure SeTOP (Figure S3B). Hence, the transformation of SeTOP to SeDPP was by way of Se exchange from TOP to DPP.<sup>[8]</sup> Furthermore, the consumption of free TOP in Equation (2) favors such exchange, which provides an answer to the open question of why secondary phosphines could have a strong impact on QD syntheses (with the exchange equilibrium of Equation (3) weighted toward SeTOP). Figure 2 and Figure 3 offer the other answer, showing the production of DPP from  $\text{Cd}(\text{OAc})_2 + \text{SeDPP}$  reactions.

Accordingly, for the approach in Equation (1), with high Cd-to-Se and Se-to-TOP feed molar ratios, SeTOP is a soluble Se source for DPP. SeDPP, being much more reactive than SeTOP,<sup>[8,9,11–13]</sup> is consumed quickly by  $\text{Cd}(\text{OAc})_2$ . It is SeDPP rather than SeTOP that reacts with  $\text{Cd}(\text{OAc})_2$ , and DPP interacts with SeTOP directly rather than with  $\text{Cd}(\text{OAc})_2$ . The coordination of TOP to  $\text{Cd}(\text{OAc})_2$  (Equation (2)) moves the equilibrium of Equation (3) to the right.

We designed two reactions with pure SeTOP to demonstrate the release of TOP shown in Equation (3), taking advantage of the strong coordination of TOP to  $\text{Cd}(\text{OAc})_2$  shown in Equation (2). The two mixtures used were



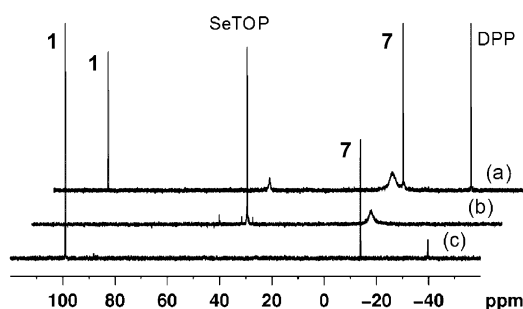


**Figure 2.**  $^{31}\text{P}$  NMR spectra from three reactions collected at 25 °C, a)  $\text{Cd}(\text{OAc})_2 + \text{SeTOP} + \text{DPP}$ , b)  $\text{Cd}(\text{OAc})_2 + \text{SeTOP}$ , and c)  $\text{Cd}(\text{OAc})_2 + \text{SeDPP}$ . See Figure S4A for in situ spectra collected at various temperatures. **1** is  $\text{C}_{17}\text{H}_{33}\text{COO-PPh}_2$  and **7** is  $\text{Ph}_2\text{P-PPh}_2$ .

$2\text{Cd}(\text{OAc})_2:1\text{SeTOP}:1.5\text{DPP}$  and  $4\text{Cd}(\text{OAc})_2:1\text{SeTOP}:1.5\text{DPP}$ . Again, the pure SeTOP made from filtering  $1.2\text{Se}:1\text{TOP}$  (90 %) did not contain any free TOP (Figure S3B, bottom). TOP coordination to  $\text{Cd}(\text{OAc})_2$  was detected by  $^{31}\text{P}$  NMR spectroscopy (Figure S3C; with more from Batch 4 $\text{Cd}(\text{OAc})_2$  than from Batch 2 $\text{Cd}(\text{OAc})_2$ ). Many more CdSe QDs were produced from Batch 4 $\text{Cd}(\text{OAc})_2$  than from the Batch 2 $\text{Cd}(\text{OAc})_2$ . High metal-to-Se and Se-to-TOP feed molar ratios should be used for the approach shown in Equation (1).<sup>[9,12,13,15]</sup>

The reaction of  $\text{Se=PPh}_2\text{H}$  and  $\text{Cd}(\text{OAc})_2$  and the ready coordination of TOP to  $\text{Cd}(\text{OAc})_2$  push the equilibrium of Equation (3) to the right. Thus, the reaction in Equation (1) affords low-temperature nucleation/growth of CdSe NCs with good yield and reproducibility. We also studied another three reactions: a)  $2.3\text{Cd}(\text{OAc})_2:1\text{SeTOP}:2.3\text{DPP}$ , b)  $2.2\text{Cd}(\text{OAc})_2:1\text{SeTOP}$ , and c)  $2.3\text{Cd}(\text{OAc})_2:1\text{SeDPP}$ . These reactions were monitored by in situ  $^{31}\text{P}$  NMR spectroscopy (Figure S4A and Figure 2). SeTOP (1M) was made with a feed molar ratio of  $1\text{Se}:2.2\text{TOP}$  (90 % pure; Figure S3B, top). SeDPP, with a feed molar ratio of  $1\text{Se}:1\text{DPP}$  contained no free DPP (Figure S4B). Compound **1**  $\text{C}_{17}\text{H}_{33}\text{COO-PPh}_2$  (approximately 98 ppm, Figure 2; labeled as **3** in Ref. [8]) and compound **7**  $\text{Ph}_2\text{P-PPh}_2$  (approximately -14 ppm; labeled as **12** in Ref. [8]) were detected in reactions (a) and (c), but not (b). Thus, the role of DPP in (a) appeared to be similar to that in (c). Note that SeDPP was not detected in reaction (c), while SeTOP was in reactions (a) and (b). Thus, SeDPP should be much more reactive than SeTOP or DPP towards  $\text{M}(\text{OAc})_2$  (where  $\text{M} = \text{Cd}, \text{Pb}, \text{or Zn}$ ).

Figure S5A shows the temporal evolution of  $^{31}\text{P}$  NMR signals of a reaction mixture of  $1\text{Cd}(\text{OAc})_2:2\text{SeDPP}$  with  $[\text{Se}]$  of  $44\text{ mmol kg}^{-1}$  in  $[\text{D}_8]\text{toluene}$ . The SeDPP used did not contain any free DPP (Figure S4B). The mixing of  $\text{Cd}(\text{OAc})_2$  and SeDPP was carried out at -78 °C (see Supporting Information for details). In situ  $^{31}\text{P}$  NMR spectra were collected from -55 °C to 100 °C and back down to 25 °C, as indicated. Unexpectedly, no SeDPP was detected at -55 °C, but DPP was detected. The coordination of 2SeDPP to  $1\text{Cd}(\text{OAc})_2$  was as we expected, together with the release of DPP. The coordination of SeDPP or SeTOP to  $\text{Cd}(\text{OAc})_2$  has been suggested but with 1:1 ratio, rather than 2:1.<sup>[6,8,10]</sup> Compounds 1–7 were detected together with DPP

( $\text{C}_{17}\text{H}_{33}\text{COO-PPh}_2$  **1**,  $\approx 98\text{ ppm}$ ;  $\text{C}_{17}\text{H}_{33}\text{COO-(Se)PPh}_2$  **3**,  $\approx 78\text{ ppm}$ ;  $\text{Ph}_2\text{P(O)OH}$  **4**,  $\approx 27\text{ ppm}$ ;  $\text{Ph}_2\text{P(O)H}$  **5**,  $\approx 22\text{ ppm}$ ; Figure S4Aa), and  $\text{Ph}_2\text{P-PPh}_2$  ( $\approx -14\text{ ppm}$ , **7**), with unknown **2** and **6**. The disproportionation reaction of a secondary phosphine oxide **5** to a secondary phosphine (DPP) and a secondary phosphinic acid **4** has been described elsewhere.<sup>[8,17]</sup> The formation of **1** and DPP has been shown in a reaction of **7** and  $\text{C}_{17}\text{H}_{33}\text{COOH}$ .<sup>[15]</sup> The absorption spectrum of the resulting CdSe NCs is shown in the right part of Figure S5A. The disappearance of SeDPP indicates a fast reaction, with the production of SeDPP (Figure S5B, collected from another two mixtures of  $1\text{Cd}(\text{OAc})_2:1\text{SeDPP}$  and  $1\text{Cd}(\text{OAc})_2:3\text{SeDPP}$ ).

Further, we studied the reactions of  $\text{Cd}(\text{OAc})_2 + \text{Se} = \text{P}(\text{CH}_3)_2\text{H}$ ,  $\text{Cd}(\text{OAc})_2 + \text{Se} = \text{PPh}_2\text{H}$ , and  $\text{Cd}(\text{OAc})_2 + \text{Se} = \text{P}(\text{CH}_3)_3$  with a computational approach, trying to identify the structures of the reactants, intermediates, transition states, and products for  $\text{Cd}(\text{OAc})_2 + \text{SeDPP}$ . For the first reaction, the release of acetic acid from a  $\text{Cd}(\text{OAc})_2(\text{Se} = \text{P}(\text{CH}_3)_2\text{H})_2$  complex (Scheme S1-1a) followed by the release of  $\text{P}(\text{CH}_3)_2\text{H}$  through  $\text{Se} = \text{P}$  bond cleavage (Scheme S1-1b) are shown in Figure 3A, with detailed calculations in Scheme S1-1. For the first step of the acid release,  $\text{Cd}(\text{OAc})_2(\text{Se} = \text{P}(\text{CH}_3)_2\text{H})_1$  and  $\text{Cd}(\text{OAc})_2(\text{Se} = \text{PPh}_2\text{H})_1$  exhibit similar pathways, with comparable activation energy of  $\Delta G = 21.00\text{ kJ mol}^{-1}$  (Scheme S1-2) and  $38.07\text{ kJ mol}^{-1}$  (Scheme S1-3), respec-

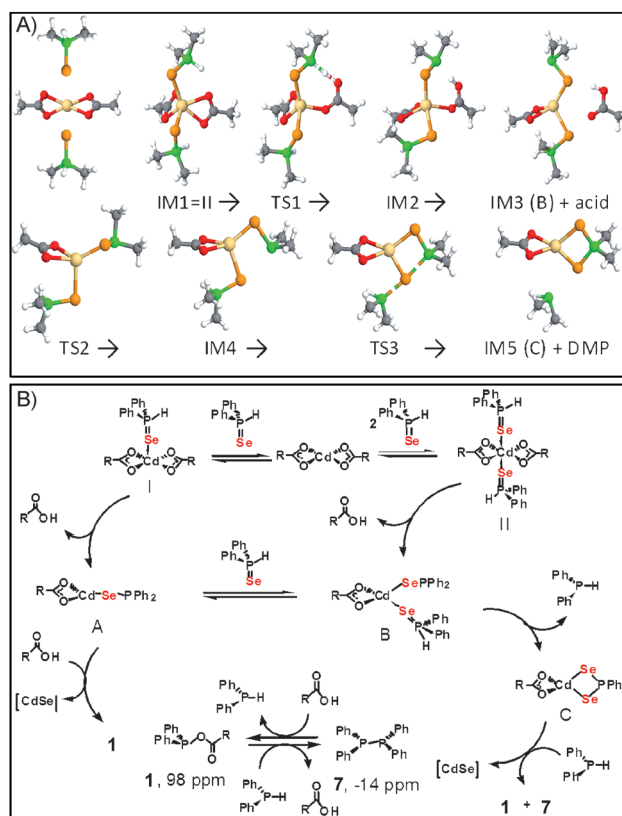


**Figure 3.** A) DFT calculations lead to a reaction pathway of  $\text{Cd}(\text{OAc})_2$  and SeDPP (Se orange, other colors same as Figure 1A). See Scheme S1 for detailed calculations. B) Proposed reaction mechanism for the reaction of  $\text{Cd}(\text{OAc})_2$  and SeDPP.

tively. Thus, it is possible to simplify  $\text{PPh}_2\text{H}$  with  $\text{P}(\text{CH}_3)_2\text{H}$  in our calculations, as confirmed by Tables S2 and S3.

Without an energy barrier, the Se atoms of two  $\text{Se}=\text{P}(\text{CH}_3)_2\text{H}$  molecules absorbed directly onto the Cd atom of  $\text{Cd}(\text{OAc})_2$  (Figure 3A). The resulting IM1 ( $\text{Cd}(\text{OAc})_2(\text{Se}=\text{P}(\text{CH}_3)_2\text{H})_2$ ) releases acetic acid, giving IM3. This pathway involves a transition state (TS1, with a  $\Delta G = 21.03 \text{ kJ mol}^{-1}$  energy barrier) of a seven-membered ring, formed by nucleophilic attack of the carboxylate on the proton of  $\text{Se}=\text{PPh}_2\text{H}$  to form one O–H bond and the breaking of one P–H bond. There are two Se–P arms bonded to the Cd atom of IM3; these two arms rotate to overcome the energy barrier of the transition state (TS2,  $\Delta G = 16.57 \text{ kJ mol}^{-1}$ ) to give IM4. Then the P atom of a  $\text{Se}-\text{P}(\text{CH}_3)_2$  arm of IM4 approaches the Se atom of a  $\text{Se}-\text{P}(\text{CH}_3)_2\text{H}$  arm, resulting in a transition state (TS3,  $\Delta G = 28.88 \text{ kJ mol}^{-1}$ ) of a P–Se–Cd–Se four-membered ring. IM5 forms after the release of  $\text{P}(\text{CH}_3)_2\text{H}$  from the  $\text{Se}-\text{P}(\text{CH}_3)_2\text{H}$  arm, with the Se–P bond cleavage.

For the formation of an CdSe monomer with the  $\text{Se}=\text{P}$  bond cleavage of  $\text{Se}=\text{P}(\text{C}_8\text{H}_{17})_3$  from reactions of  $\text{Cd}(\text{OA})_2$  and SeTOP, Alivisatos, Liu, and co-workers proposed a reaction pathway of nucleophilic attack of the carboxylate (of free  $\text{C}_{17}\text{H}_{33}\text{COOH}$ ) on the P atom of SeTOP in  $\text{Cd}(\text{OA})_2$ –(SeTOP).<sup>[10]</sup> Thus, we calculated a similar pathway (Scheme S2) showing nucleophilic attack of the carboxylate on the P atom of  $\text{Se}=\text{P}(\text{CH}_3)_2\text{H}$ . The energy barrier of the resulting transition state (TS1,  $\Delta G = 116.01 \text{ kJ mol}^{-1}$ ) of a six-membered ring is much higher than that of the acid release pathway (Scheme S1). Thus, the pathway shown in Scheme S2 is not plausible. Furthermore, for  $\text{Cd}(\text{OAc})_2(\text{Se}=\text{P}(\text{CH}_3)_3)_2$ , nucleophilic attack of the carboxylate on the P atom of  $\text{Se}=\text{P}(\text{CH}_3)_3$  was calculated (Scheme S3). The energy barrier of the transition state (TS1,  $\Delta G = 161.76 \text{ kJ mol}^{-1}$ ) of a six-membered ring is high. Therefore, without the addition of DPP, a high reaction temperature is needed for the formation of CdSe NCs from reactions of  $\text{Cd}(\text{OAc})_2$  and  $\text{Se}=\text{P}(\text{CH}_3)_3$ .

Now, it is easy to understand that with the approach from Equation (1), the formation of CdSe NCs is much easier, owing to the formation of SeDPP. SeDPP is much more reactive toward  $\text{Cd}(\text{OAc})_2$  than SeTOP. For reactions of  $\text{Cd}(\text{OA})_2$  and SeDPP, we propose a mechanism, shown in the bottom part of Figure 3. The release of RCOOH first and DPP second is noteworthy: the RCOOH release was detected by  $^1\text{H}$  NMR and  $^{13}\text{C}$  NMR spectroscopy (Figure S5C), while the DPP release could be seen clearly by  $^{31}\text{P}$  NMR spectroscopy (Figure 2c; Figures S5A and S5B at  $-55^\circ\text{C}$ ). The equilibrium of  $\text{C}_{17}\text{H}_{33}\text{COO}-\text{PPh}_2 + \text{DPP} \rightleftharpoons \text{Ph}_2\text{P}-\text{PPh}_2 + \text{RCOOH}$  exists (Figure S5D). See Scheme S4 for our step-by-step explanation of Figure 3B.

In conclusion, we demonstrated that the use of a commercial secondary phosphine  $\text{PPh}_2\text{H}$ , together with high Cd-to-Se and Se-to-TOP feed molar ratios, offers a practical means to overcome the challenges associated with the synthesis of colloidal semiconductor QDs: reaction temperature, particle yield, and synthetic reproducibility. For a model reaction of  $\text{Cd}(\text{OA})_2$  and SeTOP in ODE, the effect of a small amount of DPP added was studied by in situ experiments and DFT calculations, which provided insights into the phosphine chemistry. We found that SeDPP, instead of SeTOP, reacts

with  $\text{Cd}(\text{OA})_2$  at low temperature for  $\text{Cd}(\text{OA})_2 + \text{SeTOP} + \text{DPP}$  with high Cd-to-Se and Se-to-TOP feed molar ratios: the TOP coordination with  $\text{Cd}(\text{OA})_2$  and high SeDPP reactivity shifted the equilibrium of  $\text{SeTOP} + \text{DPP} \rightleftharpoons \text{SeDPP} + \text{TOP}$  toward SeDPP. For the  $\text{Cd}(\text{OA})_2$  and SeDPP reaction, reaction pathways were outlined showing the release of  $\text{C}_{17}\text{H}_{33}\text{COOH}$  from  $\text{Cd}(\text{OA})_2(\text{Se}=\text{PPh}_2\text{H})_2$ , followed by the release of  $\text{PPh}_2\text{H}$ . The two reactions are fast with small energy barriers. Accordingly, the presence of a small amount of secondary phosphines can play a significant role for the approach shown in Equation (1), with high Cd-to-Se and Se-to-TOP feed molar ratios. For the  $\text{Cd}(\text{OA})_2 + \text{SeDPP}$  reaction, after the release of acid and DPP, our DFT calculations suggested the presence of an intermediate  $\text{RCOO}-\text{CdSe}-\text{SePPh}_2$  (C), a diselenophosphinato complex that is a single-source precursor in nature. Thus, the approach in Equation (1) shares similar technological implications as the use of single-source precursors for various semiconductor materials including spherical NPs, nanowires, nanorods, and thin films.<sup>[22]</sup> We provided a straightforward approach for the rational design and synthesis of colloidal semiconductor NCs at low temperature, maintaining high quality, particle yield, and synthetic reproducibility.

Received: January 22, 2013

Published online: March 25, 2013

**Keywords:** density functional calculations · molecular modeling · phosphines · semiconducting nanocrystals · quantum dots

- [1] Editorial: *Nat. Nanotechnol.* **2010**, *5*, 381–381.
- [2] K. Sanderson, *Nat. Nanotechnol.* **2009**, *4*, 760–761.
- [3] C. B. Murray, D. J. Norris, M. G. Bawendi, *J. Am. Chem. Soc.* **1993**, *115*, 8706–8715.
- [4] Z. A. Peng, X. Peng, *J. Am. Chem. Soc.* **2001**, *123*, 183–184.
- [5] Y. A. Yang, H. Wu, K. R. Williams, Y. C. Cao, *Angew. Chem.* **2005**, *117*, 6870–6873; *Angew. Chem. Int. Ed.* **2005**, *44*, 6712–6715.
- [6] J. S. Steckel, B. K. H. Yen, D. C. Oertel, M. G. Bawendi, *J. Am. Chem. Soc.* **2006**, *128*, 13032–13033.
- [7] J. Joo, J. M. Pietryga, J. A. McGuire, S.-H. Jeon, D. J. Williams, H.-L. Wang, V. I. Klimov, *J. Am. Chem. Soc.* **2009**, *131*, 10620–10628.
- [8] C. M. Evans, M. E. Evans, T. D. Krauss, *J. Am. Chem. Soc.* **2010**, *132*, 10973–10975.
- [9] J. Ouyang et al., *ACS Appl. Mater. Interfaces* **2011**, *3*, 553–565, see Supporting Information.
- [10] a) H. Liu, J. S. Owen, A. P. Alivisatos, *J. Am. Chem. Soc.* **2007**, *129*, 305–312; b) R. García-Rodríguez, H. Liu, *J. Am. Chem. Soc.* **2012**, *134*, 1400–1403.
- [11] a) B. M. Cossairt, J. S. Owen, *Chem. Mater.* **2011**, *23*, 3114–3119; b) K. Yu, *Adv. Mater.* **2012**, *24*, 1123–1132.
- [12] K. Yu, J. Ouyang, D. M. Leek, *Small* **2011**, *7*, 2250–2262.
- [13] K. Yu, A. Hrdina, X. Zhang, J. Ouyang, D. M. Leek, X. Wu, M. Gong, D. Wilkinson, C. Li, *Chem. Commun.* **2011**, *47*, 8811–8813.
- [14] a) W. Ma, J. M. Luther, H. Zheng, Y. Wu, A. P. Alivisatos, *Nano Lett.* **2009**, *9*, 1699–1703; b) K. Yu et al., *ACS Appl. Mater. Interfaces* **2011**, *3*, 1511–1520, see Supporting Information.
- [15] K. Yu, A. Hrdina, J. Ouyang, D. Kingston, X. Wu, D. M. Leek, X. Liu, C. Li, *ACS Appl. Mater. Interfaces* **2012**, *4*, 4302–4311.

- [16] K. Yu et al., *ACS Appl. Mater. Interfaces* **2013**, DOI: 10.1021/am302951k, see Supporting Information.
- [17] F. Wang, W. R. Buhro, *J. Am. Chem. Soc.* **2012**, *134*, 5369–5380.
- [18] B. K. Hughes, J. M. Luther, M. C. Beard, *ACS Nano* **2012**, *6*, 4573–4579.
- [19] L. M. Jackman, F. A. Cotton, *Dynamic Nuclear Magnetic Resonance Spectroscopy*, Academic Press, New York, **1975**.
- [20] W. Yang, R. G. Parr, *Proc. Natl. Acad. Sci. USA* **1985**, *82*, 6723–6726.
- [21] Y. Li, J. N. S. Evans, *J. Am. Chem. Soc.* **1995**, *117*, 7756–7759.
- [22] M. A. Malik, M. Afzaal, P. O'Brien, *Chem. Rev.* **2010**, *110*, 4417–4446.
-